J. Fluid Mech. (1987), *vol.* 179, *pp.* 201–225
Printed in Great Britain

Shear-flow instability due to a wall and a viscosity discontinuity at the interface

By A. P. HOOPER AND W. G. C. BOYD
Department of Mathematics, University of Bristol, Bristol BS8 1TW, UK

(Received 5 December 1985 and in revised form 24 October 1986)

Consider the Couette flow of two superposed fluids of different viscosity with the depth of the lower fluid bounded by a wall and the interface while the depth of the upper fluid is unbounded. The linear instability of this flow configuration is studied at all values of flow Reynolds number and disturbance wavelength using both asymptotic and numerical methods. Three distinct forms of instability are found which are dependent on the magnitude of two dimensionless parameters β and $(\alpha R)^{\frac{1}{3}}$, where β is a dimensionless wavenumber measured on a viscous lengthscale, α is a dimensionless wavenumber measured on the scale of the depth of the lower fluid and R is the Reynolds number of the lower fluid. At large β there is the short-wave instability found previously by Hooper & Boyd (1983). At small β and small $(\alpha R)^{\frac{1}{3}}$ there is the long-wave instability first discovered by Yih. At small β and large $(\alpha R)^{\frac{1}{3}}$ there is a new type of instability which arises only if the kinematic viscosity of the lower bounded fluid is less than the kinematic viscosity of the upper fluid.

1. Introduction

It is known that the viscosity discontinuity at the interface between two viscous fluids in shearing motion can cause instability, Yih (1967), Hooper & Boyd (1983, hereinafter referred to as HB). HB studied the Couette flow of two superposed viscous fluids in an infinite region – that is, in the absence of solid boundaries – and showed that the flow was always unstable. Remarkably the instability was in essence a short-wave instability. In contrast, Yih, who studied plane Couette and plane Poiseuille flow of two superposed fluids of different viscosity confined to a channel, showed that instability may exist in the long-wavelength limit. In this paper we study the instability at all wavelengths of a flow intermediate between those two.

The flow we study is that of two superposed viscous fluids in linear shearing motion bounded by one wall (see figure 1). We find that, in addition to the Yih-type and HB instabilities, there is a new type which arises at large Reynolds number and is due to the effect of the viscous boundary layer at the wall on the inviscid flows that can exist on either side of the interface.

Its growth rate is determined by the ratio of the viscosities and densities of the two fluids and the depth of the lower bounded fluid. Equation (3.32*c*) of §3.2 shows that the flow can be unstable if the kinematic viscosity of the lower bounded fluid is less than the kinematic viscosity of the upper fluid. (It is only in §3.2 that we consider fluids of unequal density and study the effect of a density stratification on the stability of the flow. Throughout the remainder of the paper we consider fluids of equal density and study only the effect of a viscosity stratification on the stability of the flow.)

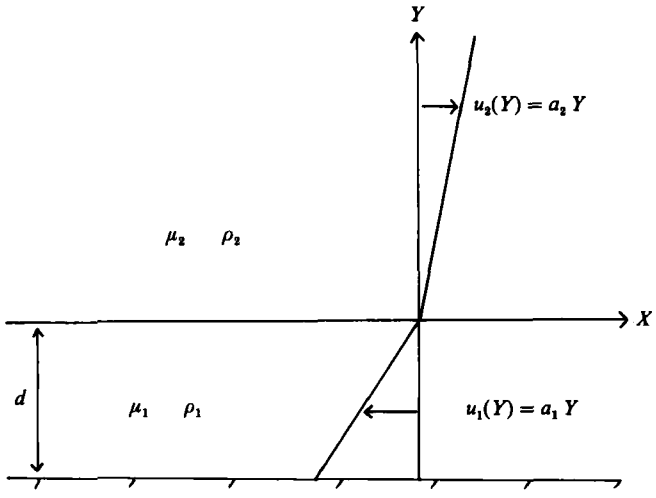

FIGURE 1. The flow configuration.

We shall find that the analysis of the linear stability problem depends on three important lengthscales: d, the distance from the wall to the interface; λ, the wavelength of the disturbance; and l, a viscous lengthscale of the disturbance. The viscous lengthscale l equals $(\lambda\nu/a)^{\frac{1}{3}}$ where ν is the kinematic viscosity and a is the shear rate of the lower bounded fluid. This lengthscale arises naturally in the linearized equations for the disturbance.

Corresponding to these three lengthscales are three dimensionless ratios:

$$\alpha = 2\pi \frac{d}{\lambda},$$

$$(\alpha R)^{\frac{1}{3}} = (2\pi)^{\frac{1}{3}} \frac{d}{l}$$

and

$$\beta = (2\pi)^{\frac{2}{3}} \frac{l}{\lambda} = \frac{\alpha}{(\alpha R)^{\frac{1}{3}}}.$$

Here R is the Reynolds number of the lower fluid, $\beta^{\frac{3}{2}}$ is the wavenumber used in the HB analysis (there denoted by α). The first two of these parameters is of course widely used in hydrodynamic stability calculations (see e.g. Drazin & Reid 1981, chapter 4) but the importance of β seems not to have been widely appreciated.

The nature of the instability for the flow configuration of figure 1 is determined primarily by the magnitude of the parameters $(\alpha R)^{\frac{1}{3}}$ and β. When $(\alpha R)^{\frac{1}{3}} \gg 1$ and $\beta \gg 1$, we find the short-wave interfacial instability of HB. A similar kind of instability is found at all values of $(\alpha R)^{\frac{1}{3}} \ll 1$ as long as $\beta \gg 1$. When $(\alpha R)^{\frac{1}{3}} \ll 1$ and $\beta \ll 1$ we find the long-wave instability similar to that found by Yih for Couette flow of two viscous fluids in a channel. Yih's analysis has been extended by Hooper (1985) to include the configuration of figure 1. Hooper found that the flow is unstable if the unbounded fluid is also the less viscous fluid. Otherwise the flow is stable. The numerical results show that this type of instability persists at zero Reynolds number (see figure 6). Surface tension stabilizes the flow and asymptotic results show that when the dimensionless surface tension S equals or exceeds 0.00498 (where S is defined

in §2) the flow is completely stable at zero R. When $(\alpha R)^{\frac{1}{3}} \gg 1$ and $\beta \ll 1$ we find the new type of instability which is due to a viscous boundary layer at the wall. When both fluids are of equal density the growth rate of this instability is determined by the ratio of the viscosities of the two fluids. If the unbounded fluid is also the more viscous fluid then the flow is unstable and vice versa.

The problem is formulated in §2. In §3 we describe a singular perturbation scheme which is used to find this new instability that occurs when $(\alpha R)^{\frac{1}{3}} \gg 1$ and $\beta \ll 1$. In §4 we derive the exact secular equation and solve for c numerically. Four different asymptotic regimes are identified according to the magnitude of $(\alpha R)^{\frac{1}{3}}$ and β, and the asymptotic analysis for the two regimes, which have not been discussed previously by HB or Yih, are described. A discussion of the results in the light of previous theoretical and experimental studies is given in §5.

2. Formulation of the problem

The basic flow configuration is shown in figure 1. The equations of motion are non-dimensionalized with respect to d, the distance from the wall to the interface and a_1, the shear rate of the lower fluid. This introduces the following dimensionless parameters:

$$R = a_1 d^2/\nu_1, \quad \text{the Reynolds number of the lower fluid,}$$

$$m = \mu_2/\mu_1, \quad \text{the viscosity ratio,}$$

$$r = \rho_2/\rho_1, \quad \text{the density ratio,}$$

$$S = T/\rho_1 a_1^2 d^3, \quad \text{the dimensionless surface tension parameter}$$

and $F = (1-r)gd/a_1^2 d^2$,

and a dimensionless coordinate system defined by

$$(x, y) = (X, Y)/d$$

where (X, Y) are denoted in figure 1.

We assume the disturbance has an x- and t-dependence of the form $\exp(\mathrm{i}\alpha(x-ct))$, where α is the dimensionless velocity of the disturbance in the x-direction. The growth rate of the disturbance is given by $\mathrm{Im}(\alpha c)$.

Therefore we find that the stream function in each fluid satisfies the Orr–Sommerfeld equations

$$\left(\frac{\mathrm{d}^2}{\mathrm{d}y^2}-\alpha^2\right)^2 \phi_1(y) = \mathrm{i}\alpha R(y-c)\left(\frac{\mathrm{d}^2}{\mathrm{d}y^2}-\alpha^2\right)\phi_1(y) \quad \text{for } -1 < y < 0, \tag{2.1a}$$

and

$$\left(\frac{\mathrm{d}^2}{\mathrm{d}y^2}-\alpha^2\right)^2 \phi_2(y) = \frac{\mathrm{i}\alpha R r}{m^2}(y-mc)\left(\frac{\mathrm{d}^2}{\mathrm{d}y^2}-\alpha^2\right)\phi_2(y) \quad \text{for } y > 0, \tag{2.1b}$$

subject to the no-slip conditions at the boundary $y = -1$,

$$\phi_1(-1) = 0, \tag{2.2a}$$

$$\frac{\mathrm{d}\phi_1}{\mathrm{d}y}(-1) = 0 \tag{2.2b}$$

and the boundedness of the disturbance as $y \to \infty$.

The boundary conditions at the interface are that each component of velocity and stress is continuous. Thus we require on $y = 0$ that

$$\phi_1 = \phi_2 = \phi(0), \tag{2.3a}$$

$$\frac{\mathrm{d}\phi_1}{\mathrm{d}y} = \frac{\mathrm{d}\phi_2}{\mathrm{d}y} + \frac{\phi(0)}{c}\frac{(1-m)}{m}, \tag{2.3b}$$

$$\left(\frac{\mathrm{d}^2}{\mathrm{d}y^2}+\alpha^2\right)\phi_1 = m\left(\frac{\mathrm{d}^2}{\mathrm{d}y^2}+\alpha^2\right)\phi_2, \tag{2.3c}$$

$$c\frac{\mathrm{d}\phi_1}{\mathrm{d}y}+\phi(0)+\frac{1}{\mathrm{i}\alpha R}\left(\frac{\mathrm{d}^2}{\mathrm{d}y^2}-3\alpha^2\right)\frac{\mathrm{d}\phi_1}{\mathrm{d}y}$$
$$= r\left(c\frac{\mathrm{d}\phi_2}{\mathrm{d}y}+\frac{\phi(0)}{m}\right)+(\alpha^2 S+F)\frac{\phi(0)}{c}+\frac{m}{\mathrm{i}\alpha R}\left(\frac{\mathrm{d}^2}{\mathrm{d}y^2}-3\alpha^2\right)\frac{\mathrm{d}\phi_2}{\mathrm{d}y}. \tag{2.3d}$$

For further details, see Yih (1967).

In §§3 and 4 we wish to compare some results with those given by HB for different values of dimensionless surface tension. We denote the dimensionless surface tension parameter of HB as S_{HB} and note that $S_{\mathrm{HB}} = SR^{\frac{2}{3}}$. Similarly we introduce the dimensionless number F_{HB} where $F_{\mathrm{HB}} = FR^{\frac{1}{3}}$. The parameters S_{HB} and F_{HB} are independent of the depth of the lower fluid d.

3. A singular perturbation scheme valid when $(\alpha R)^{\frac{1}{3}} \gg 1$ and $\beta \ll 1$

When $(\alpha R)^{\frac{1}{3}} \gg 1$ and $\beta \ll 1$, the viscous lengthscale of the disturbance l is much less than the distance between the wall and the interface d and the wavelength of the disturbance λ. We can therefore argue that within most of fluids 1 and 2 viscous forces are much less important than inviscid or inertial forces and may be neglected. In some regions, however, viscous forces may be of the same order of magnitude as the inertial forces. These regions are the viscous boundary layer at the wall, the viscous boundary layer at the interface and the critical layer where the velocity of the disturbance equals the basic flow velocity. The solution to the problem defined in §2 can therefore be found by a singular perturbation scheme, which is described below for the case $r = 1$ and $S = 0$.

3.1. *The singular perturbation scheme*

When $(\alpha R)^{\frac{1}{3}} \gg 1$ and $\beta \ll 1$, the viscous part of the Orr–Sommerfeld equation (left-hand side of (2.1)) may be neglected except within the viscous boundary layers at the wall and interface and the critical layer. Thus outside these layers the eigenfunctions ϕ_1 and ϕ_2 both satisfy

$$\left(\frac{\mathrm{d}^2}{\mathrm{d}y^2}-\alpha^2\right)\phi = 0, \tag{3.1}$$

which gives
$$\phi_1^{(0)} = b_{00}\,\mathrm{e}^{-\alpha y} + d_{00}\,\mathrm{e}^{\alpha y} \tag{3.2a}$$

and
$$\phi_2^{(0)} = a_{00}\,\mathrm{e}^{-\alpha y} \tag{3.2b}$$

since ϕ_2 is bounded as $y \to \infty$.

Fluid 1 is bounded by a wall at $y = -1$ and hence ϕ_1 contains an inner solution

$\phi_1^{(w)}$ valid within the viscous boundary layer near $y = -1$. To find this inner solution, we transform (2.1a) by the change of variable

$$z = (\alpha R)^{\frac{1}{3}}(1+y) \tag{3.3}$$

to give

$$\frac{d^2\omega_1}{dz^2} = \left[-i(1+c)+i\frac{z}{(\alpha R)^{\frac{1}{3}}}+\frac{\alpha^2}{\alpha R}\right]\omega_1, \tag{3.4a}$$

where

$$\omega_1 = \left(\frac{d^2}{dz^2}-\frac{\alpha^2}{\alpha R}\right)\phi_1^{(w)}. \tag{3.4b}$$

The form of (3.4) suggests an expansion for ω_1, $\phi_1^{(w)}$ and c of the form

$$\omega_1 = \sum_{n=0}^{\infty}\left(\frac{1}{(\alpha R)^{\frac{1}{3}}}\right)^n \omega_{1n}, \tag{3.5a}$$

$$\phi_1^{(w)} = \sum_{n=0}^{\infty}\left(\frac{1}{(\alpha R)^{\frac{1}{3}}}\right)^n \phi_{1n}^{(w)} \tag{3.5b}$$

and

$$c = \sum_{n=0}^{\infty}\left(\frac{1}{(\alpha R)^{\frac{1}{3}}}\right)^n c_n, \tag{3.5c}$$

where ω_{1n} satisfies

$$\left(\frac{d^2}{dz^2}+i(1+c_0)\right)\omega_{1n} = iz\omega_{1(n-1)} - i\sum_{j=1} c_j\omega_{1(n-j)} + \alpha^2\omega_{1(n-2)}, \tag{3.6a}$$

and $\phi_{1n}^{(w)}$ satisfies

$$\left(\frac{d^2}{dz^2}-\frac{\alpha^2}{\alpha R}\right)\phi_{1n}^{(w)} = \omega_{1n}. \tag{3.6b}$$

(In (3.6a) ω_{1j} is identically zero when j is negative.)

We are thus able to find a series expansion in $(\alpha R)^{-\frac{1}{3}}$ for $\phi_1^{(w)}$ which is valid within the viscous boundary layer at the wall, $y = -1$. We match this solution to the inviscid solution for ϕ_1 (equation (3.2a)) and thus find a series expansion in $(\alpha R)^{-\frac{1}{3}}$ for $\phi_1^{(o)}$ (see (3.14a)). We assume that the critical layer is not close to either the viscous boundary layer at the wall or the viscous boundary layer at the interface. This assumption is verified *a posteriori* in (3.23). It can then be shown that the eigenfunction ϕ has the same form inside the critical layer as outside the critical layer since the velocity profile has zero curvature. Therefore the presence of the critical layer, whether it occurs within fluid 1 or fluid 2 can be ignored.

Next we find a series expansion in $(\alpha R)^{-\frac{1}{3}}$ for the eigenfunctions $\phi_j, j = 1, 2$, within the viscous boundary layer at the interface and match the inner interfacial viscous solution $\phi_j^{(i)}$ to the corresponding outer inviscid solution $\phi_j^{(o)}$, $j = 1, 2$. The eigenfunctions $\phi_j^{(i)}$ are substituted into the four interfacial conditions at $y = 0$ (equation (2.3)). We thus find a series expansion in $(\alpha R)^{-\frac{1}{3}}$ for the eigenvalue c (see (3.23)–(3.27)).

We first solve the viscous-boundary-layer equations at the wall, (3.6), at leading order. This gives a series expansion in $(\alpha R)^{-\frac{1}{3}}$ for the outer inviscid solution $\phi_1^{(o)}$ which is valid up to $O(\alpha R)^{-\frac{1}{3}}$. The boundary conditions at the interface show that the viscous boundary layer at the interface does not affect the disturbance until $O(\alpha R)^{-1}$. Therefore we can determine c up to $O(\alpha R)^{-\frac{1}{3}}$ by substituting the inviscid eigenfunctions $\phi_j^{(o)}, j = 1, 2$ into the inviscid boundary conditions at the interface – namely continuity of normal velocity and continuity of normal stress (equations (2.3a, d)).

The first two terms in the expansion for the eigenvalue c are given in (3.23)–(3.24). To determine higher-order terms of c, however, we must consider the full viscous solution of the eigenfunctions ϕ_j ($j = 1, 2$) valid within the interfacial viscous boundary layer. The eigenvalue c is then found to satisfy (3.27).

The leading-order term for $\phi_1^{(w)}$ is found from (3.6) and satisfies

$$\phi_{10}^{(w)} = d_{10} \exp[\alpha/(\alpha R)^{\frac{1}{3}} z] + b_{10} \exp[-\alpha/(\alpha R)^{\frac{1}{3}} z] + d_{1i} e^{pz} + b_{1i} e^{-pz}, \tag{3.7}$$

where

$$p = e^{-i\pi/4} (1 + c_0)^{\frac{1}{2}}. \tag{3.8}$$

We require that this leading-order solution match the outer solution in the overlap region when $1 + y \ll 1$ but $(\alpha R)^{\frac{1}{3}}(1 + y) \gg 1$. Then both the inner wall solution of (3.7) and the outer inviscid solution of (3.2a) are valid. This implies that at leading order

$$d_{1i} = 0. \tag{3.9a}$$

$$b_{00} e^{\alpha} = d_{10} \tag{3.9b}$$

and

$$d_{00} e^{-\alpha} = b_{10}. \tag{3.9c}$$

The no-slip and no-flux boundary conditions at the wall, $z = 0$,

$$\phi_{10}^{(w)}(0) = 0, \quad \frac{d\phi_{10}^{(w)}(0)}{dz} = 0 \tag{3.10a}$$

yield

$$d_{10} = \tfrac{1}{2} b_{1i} \frac{(\alpha R)^{\frac{1}{3}} p}{\alpha} \left(1 - \frac{\alpha}{(\alpha R)^{\frac{1}{3}} p}\right) \tag{3.10b}$$

and

$$b_{10} = -\tfrac{1}{2} b_{1i} \frac{(\alpha R)^{\frac{1}{3}} p}{\alpha} \left(1 + \frac{\alpha}{(\alpha R)^{\frac{1}{3}} p}\right). \tag{3.10c}$$

We substitute (3.9) and (3.10) in (3.2) to find that the outer solution for ϕ_1 may be expressed in terms of only one unknown constant and that at leading order $\phi_1^{(o)}$ satisfies

$$\phi_1^{(o)} = \bar{b}_0 \left[\sinh \alpha(1 + y) - \frac{\alpha}{(\alpha R)^{\frac{1}{3}} p} \cosh \alpha(1 + y)\right], \tag{3.11}$$

where

$$\bar{b}_0 = -b_{1i} \frac{(\alpha R)^{\frac{1}{3}} p}{\alpha}.$$

A more accurate representation for $\phi_1^{(o)}$ is found if we solve for ω_1 and $\phi_1^{(w)}$ at the next order, $O(1/(\alpha R)^{\frac{1}{3}})$. From (3.6) and (3.7) we find that

$$\phi_{11}^{(w)} = d_{11} \exp[\alpha/(\alpha R)^{\frac{1}{3}} z] + b_{11} \exp[-\alpha/(\alpha R)^{\frac{1}{3}} z] + b_{1i} \exp[-pz] (-i) \left[\frac{1}{4p} z^2 + \frac{1}{p^2} \left(\frac{5}{4} - \frac{c_1 p}{2}\right) z + \frac{2}{p^3} \left(1 - \frac{c_1 p}{2}\right)\right]. \tag{3.12}$$

The boundary conditions at $y = -1$, (3.10a), and the matching criteria in the overlap regions when $1 + y \ll 1$ yet $(\alpha R)^{\frac{1}{3}} z \gg 1$ then yield that the outer solution $\phi_1^{(o)}$ is given by

$$\phi_1^{(o)} = \bar{b}_0 \left\{\sinh \alpha(1 + y) \left[1 - \frac{i}{(\alpha R)^{\frac{1}{3}}} \frac{1}{p^3} (\tfrac{3}{4} - \tfrac{1}{2} c_1 p)\right] - \frac{\alpha}{(\alpha R)^{\frac{1}{3}} p} \cosh \alpha(1 + y) \left[1 - \frac{i}{(\alpha R)^{\frac{1}{3}}} \frac{1}{p^3} (2 - c_1 p)\right]\right\}, \tag{3.13}$$

which can be more conveniently written in the form

$$\phi_1^{(0)} = b_0\left\{\sinh\alpha(1+y)+\alpha\cosh\alpha(1+y)\left[-\frac{1}{(\alpha R)^{\frac{1}{2}}p}+\frac{\mathrm{i}}{\alpha R}\left(\frac{(\frac{5}{4}-\frac{1}{2}c_1 p)}{p^4}\right)\right]+O(\alpha R)^{-\frac{3}{2}}\right\}, \tag{3.14a}$$

where

$$b_0 = \bar{b}_0\left[1-\frac{\mathrm{i}}{(\alpha R)^{\frac{1}{2}}}\frac{1}{p^3}(\tfrac{3}{4}-\tfrac{1}{2}c_1 p)+O((\alpha R)^{-1})\right].$$

Thus the expansion in $(\alpha R)^{-\frac{1}{2}}$ for ϕ_1 within the viscous boundary layer at the wall leads to another expansion in $(\alpha R)^{-\frac{1}{2}}$ for ϕ_1 in the outer inviscid region. Similarly we see that in fluid 2, the outer inviscid solution for ϕ_2 has the form

$$\phi_2^{(0)} = \sum_{j=0}^{n} a_{0j}(\alpha R)^{-j/2}\,\mathrm{e}^{-\alpha y}. \tag{3.14b}$$

The value of c is found from the interfacial boundary conditions at $y = 0$, (2.3). Equation (3.4) is not valid near $y = 0$ because of the presence of an interfacial viscous boundary layer there where again viscous forces must be taken into account.

To find a solution for ϕ_1 and ϕ_2 valid at the interface we transform (2.1) by the change of variable

$$u = (\alpha R)^{\frac{1}{3}}y \tag{3.15}$$

to give

$$\frac{\mathrm{d}^2\omega_1}{\mathrm{d}u^2} = \left[-\mathrm{i}c+\frac{\mathrm{i}u}{(\alpha R)^{\frac{1}{3}}}+\frac{\alpha^2}{\alpha R}\right]\omega_1, \tag{3.16a}$$

$$\frac{\mathrm{d}^2\omega_2}{\mathrm{d}u^2} = \left[-\frac{\mathrm{i}c}{m}+\frac{\mathrm{i}u}{(\alpha R)^{\frac{1}{3}}m^2}+\frac{\alpha^2}{\alpha R}\right]\omega_2, \tag{3.16b}$$

where

$$\left(\frac{\mathrm{d}^2}{\mathrm{d}t^2}-\frac{\alpha^2}{\alpha R}\right)\phi_j^{(1)} = \omega_j \quad (j = 1, 2). \tag{3.16c}$$

We look for solutions to (3.16) of the form

$$\phi_j^{(1)} = \sum_{n=0}^{\infty}(\alpha R)^{-n/2}\phi_{jn}^{(1)} \quad (j = 1, 2), \tag{3.17}$$

and match the inner interfacial solution to the outer inviscid solution of (3.14) in the overlap region where $|y| \ll 1$ but $(\alpha R)^{\frac{1}{3}}|y| \gg 1$. Thus we find that near $y = 0$

$$\phi_1^{(1)} = b_0\left\{\sinh\alpha(1+y)+\alpha\cosh\alpha(1+y)\left[\frac{1}{(\alpha R)^{\frac{1}{3}}}\left(-\frac{1}{p}\right)+\frac{\mathrm{i}}{\alpha R}\left(\frac{(\frac{5}{4}-\frac{1}{2}c_1 p)}{p^4}\right)+O(\alpha R)^{-\frac{3}{2}}\right]\right\}$$
$$+\exp[q(\alpha R)^{\frac{1}{3}}y]\left(\sum_{n=0}^{\infty}d_{1n}(\alpha R)^{-n/2}\right)$$
$$\times\left\{\frac{\mathrm{i}}{4q}y^2+\frac{1}{(\alpha R)^{\frac{1}{3}}}\left[1-\frac{\mathrm{i}}{q^2}\left(\frac{5}{4}+\frac{c_1 q}{2}\right)y\right]+\frac{1}{\alpha R}\frac{2\mathrm{i}}{q^3}\left(1+\frac{c_1 q}{2}\right)+O(\alpha R)^{-\frac{3}{2}}\right\} \tag{3.18a}$$

and

$$\phi_2^{(1)} = \mathrm{e}^{-\alpha y}\left(\sum_{n=0}^{\infty}a_{0n}(\alpha R)^{-n/2}\right)+\exp[-q(\alpha R)^{\frac{1}{3}}y/m^{\frac{1}{3}}]\left(\sum_{n=0}^{\infty}b_{1n}(\alpha R)^{-n/2}\right)$$
$$\times\left\{-\frac{\mathrm{i}}{4q}\frac{m^{\frac{1}{3}}y^2}{m^2}+\frac{1}{(\alpha R)^{\frac{1}{3}}}\left[1-\frac{\mathrm{i}m}{q^2}\left(\frac{5}{4m^2}-\frac{c_1 q}{2m^{\frac{3}{2}}}\right)y\right]-\frac{1}{\alpha R}\frac{2\mathrm{i}m^{\frac{2}{3}}}{q^3}\left(\frac{1}{m^2}-\frac{c_1 q}{2m^{\frac{3}{2}}}\right)+O(\alpha R)^{-\frac{3}{2}}\right\}, \tag{3.18b}$$

where

$$q = \mathrm{e}^{-\mathrm{i}\pi/4}c_0^{\frac{1}{3}} \quad \text{or} \quad \mathrm{e}^{\mathrm{i}\pi/4}(-c_0)^{\frac{1}{3}}. \tag{3.19}$$

(The constants d_{in} and b_{in} of (3.18) should not be confused with the constants d_{ij}, b_{ij}, $j = 0, 1$ or d_{1i} and b_{1i} of (3.7), (3.12).) The interfacial boundary conditions (2.3) at leading order are

$$b_0 \sinh\alpha = a_{00}, \tag{3.20a}$$

$$qd_{i0} = -\frac{q}{m^{\frac{1}{2}}} b_{i0}, \tag{3.20b}$$

$$q^2(\alpha R)\, d_{i0} = m\frac{q^2}{m}(\alpha R)\, b_{i0}, \tag{3.20c}$$

$$q^3(\alpha R)^{\frac{1}{2}} d_{i0} = m\left(\frac{-q^3}{m^{\frac{3}{2}}}\right)(\alpha R)^{\frac{1}{2}} b_{i0}. \tag{3.20d}$$

Equations (3.20b, c, d) combine to give

$$d_{i0} = b_{i0} = 0.$$

Therefore the leading-order terms of (2.3b, c, d) are

$$\alpha b_0 \cosh\alpha + qd_{i1} = -\alpha a_{00} - \frac{q}{m^{\frac{1}{2}}} b_{i1} + \frac{a_{00}}{c_0}\frac{(1-m)}{m}, \tag{3.21a}$$

$$q^2(\alpha R)^{\frac{1}{2}} d_{i1} = m\frac{q^2}{m}(\alpha R)^{\frac{1}{2}} b_{i1}, \tag{3.21b}$$

$$c_0(\alpha b_0 \cosh\alpha + qd_{i1}) + q^3 d_{i1} = c_0\left(-\alpha a_{00} - \frac{q}{m^{\frac{1}{2}}} b_{i1}\right) + a_{00}\left(\frac{1-m}{m}\right) - m\frac{q^3}{m^{\frac{3}{2}}} b_{i1}. \tag{3.21c}$$

These equations show that

$$d_{i1} = b_{i1} = 0. \tag{3.22}$$

Then (3.21a), the tangential velocity condition, is equivalent to (3.21c), the normal stress condition. From (3.20a), the normal velocity condition, and (3.21a) or (3.21c) we find that

$$c_0 = \frac{1-m}{m}\left[\frac{1-\mathrm{e}^{-2\alpha}}{2\alpha}\right]. \tag{3.23}$$

Thus at leading order the viscous portion of the disturbance at the interface is negligible and the first term in the series expansion for c, (3.5c), is found from the solution of the inviscid boundary conditions at the interface, which are continuity of normal velocity and stress.

The interfacial boundary conditions at next order yield

$$a_{01} = b_0 \cosh\left(-\frac{1}{p}\right), \tag{3.24a}$$

$$d_{i2} = -m^{-\frac{1}{2}} b_{i2} \tag{3.24b}$$

where

$$b_{i2} = 2\alpha^2 \frac{b_0(1-m)\, m^{\frac{1}{2}}}{q^2(1+m^{\frac{1}{2}})} \sinh\alpha \tag{3.24c}$$

and

$$c_1 = -\frac{(1-m)}{m}\frac{\mathrm{e}^{-2\alpha}}{p}. \tag{3.24d}$$

Since
$$p = e^{-i\pi/4}(1+c_0)^{\frac{1}{2}},$$
$$c_1 = -\frac{(1-m)}{m} e^{i\pi/4} \frac{e^{-2\alpha}}{(1+c_0)^{\frac{1}{2}}}, \tag{3.25}$$

which implies that the flow is unstable if $m > 1$ and stable otherwise.

One may proceed in a similar fashion to calculate higher-order approximations to c. We find that the inviscid part of the eigenfunctions $\phi_1^{(i)}$ and $\phi_2^{(i)}$ contribute a second-order correction to c of the form

$$c_{2i} = -i\left(\frac{1-m}{m}\right) e^{-2\alpha} \frac{[\frac{5}{4}+\frac{1}{2}(1-m/m)\, e^{-2\alpha}+\alpha(1+c_0)]}{(1+c_0)^2}, \tag{3.26a}$$

and the viscous part of $\phi_1^{(i)}$ and $\phi_2^{(i)}$ contribute a second-order connection to c of the form

$$c_{2v} = -2i\alpha^2[(1+m)+(1-m)\, e^{-2\alpha}]. \tag{3.26b}$$

We thus have found an expansion for c of the form

$$c = c_0+\frac{1}{(\alpha R)^{\frac{1}{2}}} c_1+\frac{1}{\alpha R}(c_{2i}+c_{2v})+\ldots, \tag{3.27}$$

where c_0 is given in (3.23), c_1 in (3.25) and c_{2i} and c_{2v} in (3.26).

This series expansion for c has been checked numerically. In §4 the exact secular equation for c is derived and solved using both numerical and asymptotic techniques. The same asymptotic expansion for c is found when $\beta \ll 1$ and $(\alpha R)^{\frac{1}{3}} \gg 1$ and the expansion is shown to be in good agreement with numerical results (see figure 4).

We note that the terms c_0, c_1 and c_{2i} all arise from the expansion for ϕ in the inviscid region and hence are due to the disturbance vorticity created at the wall. The term c_0 is real and therefore does not affect the stability of the flow. The imaginary part of both c_1 and c_{2i} is positive when $m > 1$ which implies that the viscous boundary layer at the wall can be a destabilizing influence on the flow.

The term c_{2v} arises from the expansion for ϕ in the viscous boundary layer near the interface. This term is pure imaginary and always negative and we therefore conclude that when $\beta \ll 1$ and $(\alpha R)^{\frac{1}{3}} \gg 1$ the viscous boundary layer at the interface has a stabilizing effect on the flow.

As $\alpha \to \infty$, c tends to the value found by Hooper & Boyd when their wavenumber was small (HB, equation (27)). Thus as the separation between the solid boundary and the interface increases with all other parameters of the flow held fixed, the destabilizing effect of the viscous boundary layer at the wall is reduced and the stability of the flow is eventually governed only by the effect of the disturbance within the viscous boundary layer at the interface. Neutral stability results when the destabilizing effect of the wall viscous boundary layer balances the stabilizing effect of the interfacial boundary layer. Therefore when $(\alpha R)^{\frac{1}{3}} \gg 1$, neutral stability will result for $m > 1$ whenever

$$\left(\frac{m-1}{m}\right) \frac{e^{-2\alpha}}{(2(1+c_0)\alpha R)^{\frac{1}{2}}} = \frac{2\alpha^2}{\alpha R}[(1+m)+(1-m)\, e^{-2\alpha}]. \tag{3.28}$$

From this equation we deduce that when $m > 1$ there exists a branch of the neutral stability curve which in the (α, R)-plane behaves like

$$\alpha \sim \tfrac{1}{4}\ln R \quad \text{as } (\alpha R)^{\frac{1}{3}} \to \infty, \tag{3.29a}$$

and in the $(\beta, (\alpha R)^{\frac{1}{3}})$-plane behaves like

$$\beta \sim \frac{\ln (\alpha R)^{\frac{1}{3}}}{(\alpha R)^{\frac{1}{3}}} \quad \text{as } (\alpha R)^{\frac{1}{3}} \to \infty. \tag{3.29b}$$

Comparison of the numerical results with (3.29) reveals that in figure 6, the appropriate branch of the neutral stability curve has not yet reached this asymptotic regime. In fact when $R = 900$ the value of $(\alpha R)^{\frac{1}{3}}$ on the appropriate neutral-stability-curve branch is only 7.86. Figure 3 clearly shows that $(\alpha R)^{\frac{1}{3}} = 7.86$ is outside the regime of this asymptotic analysis. The numerical results show that the appropriate branch of the neutral stability curve approaches the asymptotic behaviour of (3.29) for $(\alpha R)^{\frac{1}{3}} \geqslant 20$ approximately.

3.2. *Unequal density and non-zero surface tension*

When the densities of fluids 1 and 2 are not equal, the eigenfunction ϕ_2 and the normal stress boundary condition must be modified to include the density ratio parameter r, where $r \neq 1$. The normal stress boundary condition must also be modified to include the effect of the gravity component acting normally to the flow and the effect of non-zero surface tension.

First we assume that surface-tension effects and gravity are negligible. When $r \neq 1$, the eigenfunction $\phi_2^{(\mathrm{i})}$, (3.18*b*), is modified to

$$\begin{aligned}\phi_2^{(\mathrm{i})} = \mathrm{e}^{-\alpha y}\left(\sum_{n=0}^{\infty} a_{0n}(\alpha R)^{-n/2}\right) + \exp\left[-q\frac{r^{\frac{1}{2}}(\alpha R)^{\frac{1}{2}}}{m^{\frac{1}{2}}}y\right]\left(\sum_{n=0}^{\infty} b_{in}(\alpha R)^{-n/2}\right) \\ \times\left\{\frac{-\mathrm{i}}{4q}\frac{r^{\frac{1}{2}}}{m^{\frac{3}{2}}}y^2 + \frac{1}{(\alpha R)^{\frac{1}{2}}}\left[1 - \frac{\mathrm{i}m}{q^2 r}\left(\frac{5r}{4m^2} - \frac{c_1 r^{\frac{3}{2}}q}{2m^{\frac{3}{2}}}\right)y\right] - \frac{1}{(\alpha R)}\frac{2\mathrm{i}m^{\frac{3}{2}}}{qr^{\frac{3}{2}}}\left(\frac{r}{m^2} - \frac{c_1 r^{\frac{3}{2}}q}{2m^{\frac{3}{2}}}\right) + O(\alpha R)^{-\frac{3}{2}}\right\}.\end{aligned} \tag{3.30}$$

The eigenfunction $\phi_1^{(\mathrm{i})}$ is unchanged.

We substitute $\phi_1^{(\mathrm{i})}$ of (3.18*a*) and $\phi_2^{(\mathrm{i})}$ of (3.30) into the interfacial boundary conditions at $y = 0$ to find that at leading order

$$b_{i0} = d_{i0} = 0, \quad a_{00} = b_0 \sinh\alpha \tag{3.31a,b}$$

and

$$c_0 = \frac{r-m}{m\alpha}\left[\frac{1}{r+\coth\alpha}\right]. \tag{3.31c}$$

At $O(\alpha R)^{-\frac{1}{2}}$

$$d_{i1} = rb_{i1} = \frac{\alpha b_0(1-r)\,r\,(\cosh\alpha + m\sinh\alpha)}{q(r-m)\,(r+r^{\frac{1}{2}}/m^{\frac{1}{3}})}, \tag{3.32a}$$

$$a_{01} = \alpha\cosh\alpha\left(-\frac{1}{p}\right)b_0 + \left(\frac{r-1}{r}\right)d_{i1} \tag{3.32b}$$

and

$$c_1 = -\frac{(r-m)}{m}\left[\frac{1}{p(\cosh\alpha + r\sinh\alpha)^2}\right] - \frac{r(1-r)^2}{qm(r-m)}\frac{(\cosh\alpha + m\sinh\alpha)^2}{(\cosh\alpha + r\sinh\alpha)^2}\frac{1}{(r+r^{\frac{1}{2}}/m^{\frac{1}{2}})}, \tag{3.32c}$$

where p is defined in (3.8) and q is defined in (3.19).

The first term in (3.32*c*) is a straightforward modification of c_1 in (3.24) and is due to the viscous boundary layer at the wall. This term is destabilizing when $r < m$ and stabilizing when $r > m$. The second term in (3.32*c*) is due to the viscous boundary

layer at the interface and is always stabilizing. Thus when $r \neq 1$, the stabilizing effect of the interfacial viscous boundary layer when $(\alpha R)^{\frac{1}{3}} \gg 1$ and $\beta \ll 1$ is apparent at $O(\alpha R)^{-\frac{1}{2}}$, compared to $O(\alpha R)^{-1}$ when $r = 1$.

When $\alpha \gg 1$, the result in (3.32) can be compared with that of Dore (1978*a*, *b*) who studied damping of interfacial gravity waves in deep water when there is no basic shear flow. He found that the interfacial viscous boundary layer introduces a stabilizing item at $O(\alpha R)^{-\frac{1}{2}}$ even when $r = 1$.

Now consider the effect of non-zero surface tension and gravity. From §2 we note that surface tension and gravity appear in the normal stress condition in the form

$$(\alpha^2 S + F)\frac{\phi(0)}{c} \tag{3.33a}$$

which equals

$$(\beta^{\frac{3}{2}} S_{\mathrm{HB}} + \beta^{\frac{3}{2}} F_{\mathrm{HB}})\frac{\phi(0)}{\alpha c}, \tag{3.33b}$$

where S, F, S_{HB} and F_{HB} are defined in §2.

Since $\beta \ll 1$, the effect of a non-zero value of S_{HB} and F_{HB} is small. The leading term is the expansion for αc is merely modified by the addition of the term

$$\left(\frac{m}{r-m}\right)(\beta^{\frac{3}{2}} S_{\mathrm{HB}} + \beta^{\frac{3}{2}} F_{\mathrm{HB}}). \tag{3.34}$$

This term is purely real and plays no part in the stability of the flow except where the leading term in the expansion for c, c_0 occurs in the next-order terms. The numerical results given in figure 3(*c*) for different values of S_{HB} confirm that in this region where $\beta \ll 1$ and $(\alpha R)^{\frac{1}{3}} \gg 1$, surface-tension effects are negligible.

3.3. *Extension to channel flow configurations*

This scheme is easily extended to channel flow configurations. Consider Couette flow of two viscous fluids of equal density confined to a channel where d_j denotes the depth of fluid j $(j = 1, 2)$. This system contains the dimensionless parameter n, the depth ratio equal to d_2/d_1 in addition to the dimensionless parameters listed in §2.

The outer inviscid solution for ϕ_2 is now affected by the viscous boundary layer that exists near the solid boundary at $y = n$ but the solution for ϕ at the interface remains unchanged. We find that the outer inviscid solution for ϕ_2 is

$$\phi_2^{(0)} = a_0 \mathrm{e}^{-\alpha y} + e_0 \mathrm{e}^{\alpha y}, \tag{3.35a}$$

and the solution for ϕ_2 near the wall, $y = n$, is at leading order

$$\phi_{20}^{(\mathrm{w})} = a_{0i} \mathrm{e}^{-sz} + e_{0i} \mathrm{e}^{sz} + a_{1i} \exp\left[-\frac{\alpha}{(\alpha R)^{\frac{1}{2}}} z\right] + e_{1i} \exp\left[\frac{\alpha}{(\alpha R)^{\frac{1}{2}}} z\right], \tag{3.35b}$$

where

$$s^2 = \frac{\mathrm{i}}{m^2}(n - mc) \tag{3.35c}$$

and

$$z = (\alpha R)^{\frac{1}{2}}(n - y). \tag{3.35d}$$

We match $\phi_2^{(\mathrm{w})}$ and $\phi_2^{(0)}$ in the overlap region where both forms of ϕ_2 are valid and apply the boundary conditions at $z = 0$ (equation (3.8)) to show that at leading order

$$\phi_2^{(0)} = a_0\left[\sinh \alpha(n-y) - \frac{\alpha}{s(\alpha R)^{\frac{1}{2}}} \cosh \alpha(n-y)\right]. \tag{3.36}$$

Section 3.1 showed that $\phi_2^{(0)}$ gives the correct behaviour for the disturbance at $y = 0$ up to $O(\alpha R)^{-\frac{1}{2}}$. Thus we need only consider the inviscid boundary conditions at $y = 0$ to show that

$$c_0 = \left(\frac{1-m}{m}\right) \frac{\sinh \alpha n \sinh \alpha}{\alpha \sinh \alpha(1+n)} \tag{3.37a}$$

and

$$c_1 = -\left(\frac{1-m}{m}\right) \left[\frac{e^{i\pi/4}(1+c_0)^{-\frac{1}{2}} \sinh^2 \alpha n + e^{-i\pi/4}\, m(n-mc_0)^{-\frac{1}{2}} \sinh^2 \alpha}{\sinh^2 \alpha(1+n)}\right]. \tag{3.37b}$$

In particular when $\alpha \ll 1$

$$c_0 = \frac{1-m}{m} \frac{n}{1+n} \tag{3.38a}$$

and

$$c_1 = -\frac{(1-m)}{m} \left[\frac{m}{2n(1+n)^3 (m+n)}\right]^{\frac{1}{2}} (m^{\frac{1}{2}} + n^{\frac{5}{2}} + i(n^{\frac{5}{2}} - m^{\frac{1}{2}})). \tag{3.38b}$$

Therefore neutral stability results when $n^5 = m$. When $m > 1$, the flow is stable if $n < m^{\frac{1}{5}}$, and unstable otherwise. Thus the depth of the more viscous fluid is an important factor in this instability and the boundary which limits the depth of the more viscous fluid exerts a stabilizing influence if close enough to the interface. These results agree with those of Renardy (1985) who studied the stability of Couette flow of two superposed viscous fluids confined to a channel using numerical techniques. She chose $m = 2$ and $n = 3$ and found a region of instability when $(\alpha R)^{\frac{1}{3}} \gg 1$ and $\beta \ll 1$.

3.4. *Energetics of the flow*

Energy considerations provide a useful insight into the nature of this instability. The energy equation for the disturbance to the flow depicted in figure 1 and averaged over one wavelength of the disturbance is

$$\int_{-1}^{0} \left(\frac{\mathrm{d}}{\mathrm{d}t}(\tfrac{1}{2}(|u_1|^2 + |v_1|^2)) + \mathrm{Re}\,(u_1 v_1^*) + \frac{2\alpha}{(\alpha R)} |e_{ij}^{(1)}|^2\right) \mathrm{d}y$$
$$+ \int_{0}^{\infty} \left(\frac{\mathrm{d}}{\mathrm{d}t}(\tfrac{1}{2}(|u_2|^2 + |v_2|^2)) + \frac{1}{m} \mathrm{Re}\,(u_2 v_2^*) + \frac{2\alpha m}{(\alpha R)} |e_{ij}^{(2)}|^2\right) \mathrm{d}y$$
$$= \frac{\alpha}{(\alpha R)} |(u_1 - u_2)\, T_{12}|_{y=0}, \tag{3.39}$$

where (u_i, v_i) is the disturbance velocity in fluid i, $(i = 1, 2)$, $e_{ij}^{(k)}$ is the rate-of-strain tensor of the disturbed flow in fluid k, $(k = 1, 2)$ and T_{12} is the tangential stress at the interface, $y = 0$. (For further details compare HB.)

When $(\alpha R)^{\frac{1}{3}} \gg 1$ and $\beta \ll 1$ all terms in (3.39) can be expressed in a descending power series of $1/(\alpha R)^{\frac{1}{2}}$. We find that the Reynolds stress and the viscous dissipation in fluid 1, the fluid which is bounded by the wall at $y = -1$ and the interface at $y = 0$, are both $O((\alpha R)^{-\frac{1}{2}})$ whereas the Reynolds stress and viscous dissipation in fluid 2 and the term on the right-hand side of (3.39), which represents a transfer of energy via the tangential stress at the interface, are all $O((\alpha R)^{-1})$. Therefore the effect of the upper fluid and the tangential stress at the interface on the instability is negligible compared to the effect of the lower bounded fluid. Further analysis shows that in fluid 1 (when $S = 0$ and $r = 1$) the sum of the viscous dissipation term and the Reynolds stress term, a term which is always positive when $\alpha R \gg 1$ and $\beta \ll 1$, is

$$\left(\frac{m-1}{m}\right) \frac{\alpha^3}{(\alpha R)^{\frac{1}{2}}} \frac{|b_0|^2}{[2(1+c_0)]^{\frac{1}{2}}} \frac{\sinh \alpha}{\alpha\, e^{\alpha}},$$

where c_0 is defined in (3.13a). The above term is positive when $m > 1$ and negative when $m < 1$. Therefore when $m > 1$, the stabilizing influence of viscous dissipation is not sufficient to overcome the destabilizing effect of the Reynolds stress. When $m < 1$, however, viscous dissipation does stabilize the disturbance.

This analysis suggests that the instability at large $(\alpha R)^{\frac{1}{3}}$ is due to the disturbance vorticity generated at the solid boundary. It seems that this unstable mode is similar in nature to a Tollmien–Schlichting wave which produces instability in bounded two-dimensional parallel shear flows. Study of the energy equation shows that the instability is driven by the Reynolds stress in the lower fluid whereas the HB short-wave instability is driven by transfer of energy at the interface via the tangential stress of the disturbance. The mechanism for the instability is therefore quite different from the mechanism for the HB short-wave instability. Viscous forces dominate the HB instability and an argument for the mechanism of this instability is given by Hinch (1984) in terms of advection of the disturbance vorticity.

4. The exact solution

4.1. *The secular equation and its numerical solution*

The problem posed in §2 may also be solved exactly for any value of α and R. We will assume $r = 1$ in this section. The Orr–Sommerfeld equations of (2.1) contain solutions in terms of Airy functions. Thus the solution to (2.1a) subject to the boundary conditions of (2.2) is

$$\phi_1(y) = a_1\left[\frac{1}{\alpha}\int_{-1}^{y}\sinh\alpha(y-z)\,\mathrm{Ai}\left(\mathrm{e}^{\mathrm{i}\pi/6}(\alpha R)^{\frac{1}{3}}\left(z-c-\mathrm{i}\frac{\alpha}{R}\right)\right)\mathrm{d}z\right]$$
$$+a_2\left[\frac{1}{\alpha}\int_{-1}^{y}\sinh\alpha(y-z)\,\mathrm{Ai}\left(\mathrm{e}^{5\mathrm{i}\pi/6}(\alpha R)^{\frac{1}{3}}\left(z-c-\mathrm{i}\frac{\alpha}{R}\right)\right)\mathrm{d}z\right], \quad (4.1a)$$

and the solution to (2.1b) subject to the boundedness of ϕ_2 as $y\to\infty$ is

$$\phi_2(y) = b_1\,\mathrm{e}^{-\alpha y}+b_2\frac{1}{2\alpha}\left\{\mathrm{e}^{-\alpha y}\int_0^y \mathrm{e}^{\alpha z}\,\mathrm{Ai}\left(\mathrm{e}^{\mathrm{i}\pi/6}\left(\frac{\alpha R}{m^2}\right)^{\frac{1}{3}}\left(z-mc-\mathrm{i}\frac{\alpha m^2}{R}\right)\right)\mathrm{d}z\right.$$
$$\left.+\mathrm{e}^{\alpha y}\int_y^\infty \mathrm{e}^{-\alpha z}\,\mathrm{Ai}\left(\mathrm{e}^{\mathrm{i}\pi/6}\left(\frac{\alpha R}{m^2}\right)^{\frac{1}{3}}\left(z-mc-\mathrm{i}\frac{\alpha m^2}{R}\right)\right)\mathrm{d}z\right\}. \quad (4.1b)$$

We substitute the above forms of ϕ_1 and ϕ_2 into the interfacial boundary conditions, (2.3), to derive a secular equation $F(\alpha, R, m, c) = 0$, which may be regarded as the dispersion relation. This secular equation has the form

$$\mathrm{e}^{\mathrm{i}\pi/6}\left[P_2(A_{12}A'_{11}-\mathrm{e}^{2\mathrm{i}\pi/3}A_{11}A'_{12})+m\left(Q_{11}-\frac{1-m}{m\kappa}\frac{1}{\beta}N_{11}\right)\left(\frac{A_{12}A'_2}{m^{\frac{2}{3}}}-\mathrm{e}^{2\mathrm{i}\pi/3}A_2A'_{12}\right)\right.$$
$$\left.-m\left(Q_{12}-\frac{1-m}{m\kappa}\frac{1}{\beta}N_{12}\right)\left(\frac{A_{11}A'_2}{m^{\frac{2}{3}}}-A_2A'_{11}\right)\right]$$
$$+2\beta(1-m)\left\{P_2\left[\mathrm{e}^{\mathrm{i}\pi/6}(N_{12}A'_{11}-\mathrm{e}^{2\mathrm{i}\pi/3}N_{11}A'_{12})+\frac{1}{\kappa}(N_{12}A_{11}-N_{11}A_{12})\right.\right.$$
$$\left.+\beta(M_{12}A_{11}-M_{11}A_{12})\right]+(M_{11}N_{12}-N_{11}M_{12})m\left[\frac{\mathrm{e}^{\mathrm{i}\pi/6}A'_2}{m^{\frac{2}{3}}}+\left(\frac{1}{m\kappa}-\beta\right)A_2\right]\Big\}$$
$$+4(\beta)^3(1-m)^2P_2(N_{11}M_{12}-M_{11}N_{12})-\mathrm{i}mS_{\mathrm{HB}}\frac{\beta^{\frac{4}{3}}}{\kappa}[P_2(A_{12}N_{11}-A_{11}N_{12})$$
$$-mA_2(M_{11}N_{12}-M_{12}N_{11})] = 0, \quad (4.2a)$$

where $$\beta = \frac{\alpha}{(\alpha R)^{\frac{1}{3}}}, \quad \kappa = (\alpha R)^{\frac{1}{3}} c,$$

$$A_{11} = \mathrm{Ai}\,(\mathrm{e}^{-5\mathrm{i}\pi/6}\,(\kappa + \mathrm{i}\beta^2)), \tag{4.2b}$$

$$A_{12} = \mathrm{Ai}\,(\mathrm{e}^{-\mathrm{i}\pi/6}\,(\kappa + \mathrm{i}\beta^2)), \tag{4.2c}$$

$$A_2 = \mathrm{Ai}\left(\frac{\mathrm{e}^{-5\mathrm{i}\pi/6}}{m^{\frac{2}{3}}}\,(m\kappa + \mathrm{i}\beta^2 m^2)\right), \tag{4.2d}$$

$$N_{1j} = \int_0^{(\alpha R)^{\frac{1}{3}}} \sinh(\beta z)\,\mathrm{Ai}\,(\mathrm{e}^{\mathrm{i}\theta_j}\,(z + \kappa + \mathrm{i}\beta^2))\,\mathrm{d}z \quad (j = 1, 2), \tag{4.2e}$$

$$M_{1j} = \int_0^{(\alpha R)^{\frac{1}{3}}} \cosh(\beta z)\,\mathrm{Ai}\,(\mathrm{e}^{\mathrm{i}\theta_j}\,(z + \kappa + \mathrm{i}\beta^2))\,\mathrm{d}z \quad (j = 1, 2), \tag{4.2f}$$

$$Q_{1j} = M_{1j} + N_{1j} \quad (j = 1, 2), \tag{4.2g}$$

$$\theta_1 = -\tfrac{5}{6}\mathrm{i}\pi, \quad \theta_2 = -\tfrac{1}{6}\mathrm{i}\pi, \tag{4.2h}$$

$$P_2 = \int_0^{\infty} \mathrm{e}^{-\beta z}\,\mathrm{Ai}\left(\frac{\mathrm{e}^{\mathrm{i}\pi/6}}{m^{\frac{2}{3}}}\,(z - m\kappa - \mathrm{i}\beta^2 m^2)\right)\mathrm{d}z, \tag{4.2i}$$

and $'$ denotes the derivative.

Inspection of (4.2) shows that the important parameters of the problem are β, which is related to the dimensionless wavenumber measured on the viscous length-scale, and $(\alpha R)^{\frac{1}{3}}$. The dimensionless wavenumber α does not appear explicitly within the expression for F.

We solve the secular equation numerically. We compute the Airy functions of complex argument that appear in (4.2*a*) using an algorithm developed by Schulten, Anderson & Gordon (1979). We find the roots of the secular equation by searching for the minima of $|F|^2$ with respect to c for any given $m(\alpha R)^{\frac{1}{3}}$, β and S_{HB}. The strategy to find all the modes of the instability is similar to that used by HB. We fix the value of m and S_{HB} and find all the roots of the secular equation when $\beta \ll 1$ and $(\alpha R)^{\frac{1}{3}} \gg 1$. We then follow each mode either by fixing $(\alpha R)^{\frac{1}{3}}$ and changing β by small steps or by fixing β and changing $(\alpha R)^{\frac{1}{3}}$ by small steps.

When $(\alpha R)^{\frac{1}{3}} \gg 1$ and $\beta \ll 1$, (4.2) reduces to

$$\left(mQ_{11} - \frac{(1-m)}{\kappa}\frac{1}{\beta}N_{11}\right)\left(\frac{A_{12}A_2'}{m^{\frac{2}{3}}} - \mathrm{e}^{2\mathrm{i}\pi/3}\,A_2 A_{12}'\right)(1+\epsilon) = 0. \tag{4.3}$$

In the above equation the relative magnitude of the neglected terms of (4.2) is denoted by ϵ. Lengthy asymptotic analysis shows that $\epsilon \sim O(\beta^2(\alpha R)^{-\frac{1}{3}})$.

The different modes of the instability are easily identified from (4.3). First there are the modes which are solutions to

$$\frac{A_{12}A_2'}{m^{\frac{2}{3}}} - \mathrm{e}^{2\mathrm{i}\pi/3}\,A_2 A_{12}' = 0. \tag{4.4}$$

There are an infinite number of modes which satisfy this equation. These are interfacial modes first identified by HB (equation (25)). They showed that these modes are stable. Figure (2*a*) shows the first four interfacial modes when $\beta = 0$ and $m = 2$. These modes have been found by solving (4.2) numerically. We see that for $(\alpha R)^{\frac{1}{3}} > 5$, the first three modes are already in the asymptotic regime $(\alpha R)^{\frac{1}{3}} \gg 1$ and $\beta \ll 1$–regime (iii) discussed below–and are solutions to (4.4).

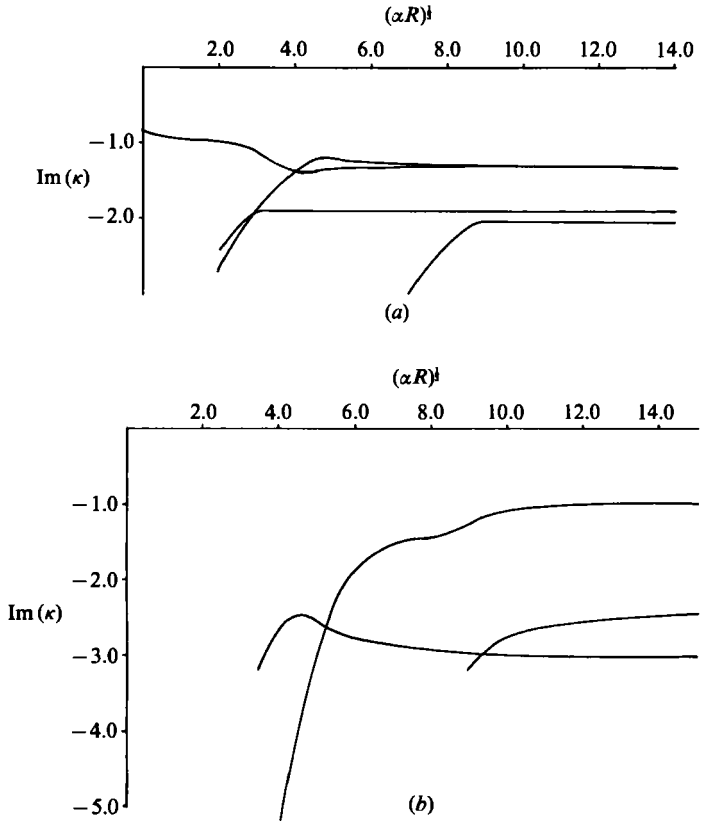

FIGURE 2. Graphs of Im (κ) *vs.* $(\alpha R)^{\frac{1}{3}}$ for $m = 2$ and $\beta = 0$ for (*a*) the interfacial modes, which for large $(\alpha R)^{\frac{1}{3}}$ are solutions to (4.4); (*b*) the wall modes, which for large $(\alpha R)^{\frac{1}{3}}$ are solutions to (4.5).

There are also modes when $Q_{11} \sim 0$ and $N_{11}/\beta \sim 0$. These are the wall modes and when $\beta = 0$ are given approximately by

$$\kappa = -(\alpha R)^{\frac{1}{3}} - z_{\pm n}\, \mathrm{e}^{-\mathrm{i}\pi/6} \quad (n = 1, 2, 3, \ldots), \tag{4.5}$$

where $z_{\pm n}$ are solutions to

$$\int_z^\infty \mathrm{Ai}\,(t)\, \mathrm{d}t = 0.$$

Figure (2*b*) shows the first three wall modes when $\beta = 0$ and $m = 2$. These modes became increasingly more difficult to compute as $(\alpha R)^{\frac{1}{3}}$ is decreased but the results suggest that they always remain stable.

There is one more mode, the solution of which is given by

$$\kappa = \frac{1-m}{m} \frac{N_{11}}{\beta Q_{11}}.$$

This mode is unstable when $m > 1$. This is precisely the same mode that is unstable in the short-wavelength regime previously studied by HB. The neutral stability curve in the $(\beta, (\alpha R)^{\frac{1}{3}})$-plane for $m = 2$ and $S_{\mathrm{HB}} = 0$ is shown in figure 3(*a*).

The asymptotic term of each branch of the neutral stability curve is marked on figure 3(*a*). The results of HB show that in the case of unbounded Couette flow,

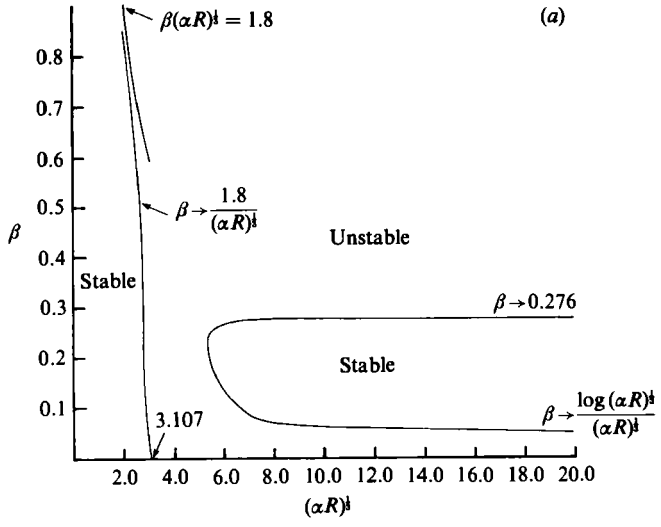

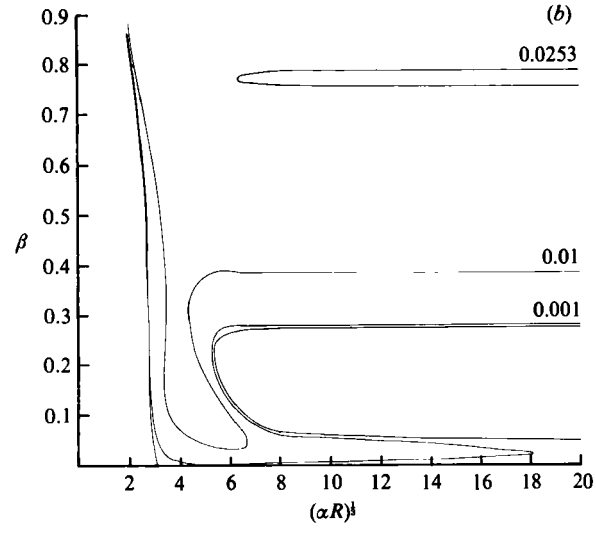

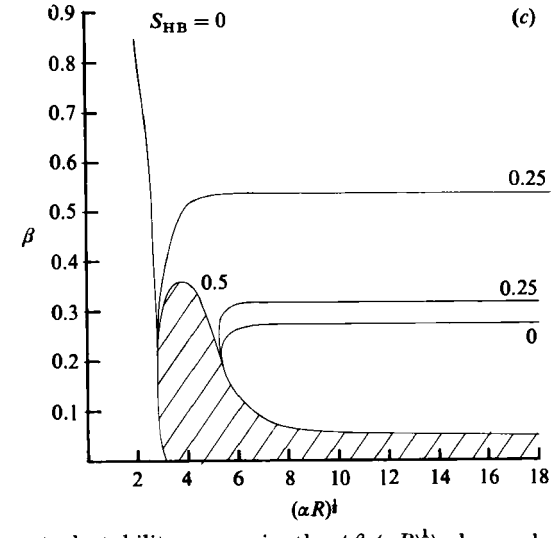

FIGURE 3. The neutral stability curve in the $(\beta, (\alpha R)^{\frac{1}{2}})$-plane when $m = 2$. (*a*) $S_{HB} = 0$. The asymptotic trend of each branch of the neutral stability curve is shown and stable and unstable regions are marked. (*b*) Lines of constant growth when $S_{HB} = 0$. The growth rate is marked on each line. (*c*) Neutral stability curve for $S_{HB} = 0$, 0.25 and 0.5. The hatched region marks the unstable region for $S_{HB} = 0.5$.

instability exists when $m = 2$ once $2\pi(\nu/a)^{\frac{1}{2}}/\lambda > 0.145$. The wavenumber β equals $[2\pi(\nu/a)^{\frac{1}{2}}/\lambda]^{\frac{2}{3}}$. Therefore we deduce from the results of HB that as $(\alpha R)^{\frac{1}{3}} \to \infty$ the upper branch of the neutral stability curve in the $(\beta, (\alpha R^{\frac{1}{3}})$-plane tends to $\beta = 0.276$. The numerical results confirm this. The asymptotic results of §3 show that as $(\alpha R)^{\frac{1}{3}} \to \infty$, the lower branch of the neutral stability curve tends to $\beta \sim \log(\alpha R)^{\frac{1}{3}}/(\alpha R)^{\frac{1}{3}}$. The other branch of the neutral stability curve, which arises in the region $(\alpha R)^{\frac{1}{3}} \sim O(1)$, is found from numerical calculations to cut the $(\alpha R)^{\frac{1}{3}}$ axis at $(\alpha R)^{\frac{1}{3}} = 3.107$. Asymptotic calculations given in §4.4 yield that as β becomes large this branch asymptotes to the hyperbola $\beta(\alpha R)^{\frac{1}{3}} = 1.8$. Figure 3(*a*) shows that the numerical results for this branch of the neutral stability curve are already quite close to the asymptotic results when $\beta \sim 1.0$.

Lines of constant growth are shown in figure 3(*b*). The regime in figure 3(*b*), where all constant-growth lines are parallel with the $(\alpha R)^{\frac{1}{3}}$ axis and are thus independent of $(\alpha R)^{\frac{1}{3}}$, can be identified with a flow configuration where the bounding wall is unimportant. Therefore we recover the results of HB. The effect of non-zero values of surface tension is shown in figure 3(*c*). The short-wave instability of HB is stabilized by surface tension. Again we recover the results of HB and show that at $m = 2.0$ and $S_{\mathrm{HB}} = 0.5$ the short-wave interfaced wave is completely stable. Surface tension, however, does not affect the instability that arises when $\beta \ll 1$.

4.2. *Asymptotic analysis of the secular equation*

We note that when $(\alpha R)^{\frac{1}{3}} \gg 1$, the integrals N_{11}, M_{11} and Q_{11} in (4.2*a*) become exponentially larger than other terms in the secular equation. If we further assume that $\beta \gg 1$ so that $N_{11} \sim \frac{1}{2}Q_{11}$ and $M_{11} \sim \frac{1}{2}Q_{11}$, we find that in the limit $(\alpha R)^{\frac{1}{3}} \to \infty$ the secular equation factorizes. One family of solutions are then given by the factor

$$Q_{11} = 0$$

and are the same modes found in semi-infinite Couette flow for short wavelengths. These modes are generated by the solid boundary and are always stable.

The second factor is identical with the secular equation found by HB for unbounded Couette flow of two superposed fluids of different viscosity and solutions to this factor are the modes generated by the presence of the interface alone. Therefore when β and $(\alpha R)^{\frac{1}{3}}$ are both large, the stability of the flow configuration of figure 1 separates into the stability problem of semi-infinite Couette flow of one fluid bounded by a wall which gives rise to stable wall modes and the stability problem of unbounded Couette flow of two superposed viscous fluids which gives rise to interfacial modes. HB have shown that one of these modes is unstable in the short-wavelength regime.

The secular equation can in fact be solved analytically if β and $(\alpha R)^{\frac{1}{3}}$ are assumed large or small. This gives rise to four regimes amenable to asymptotic investigation.

(i) $(\alpha R)^{\frac{1}{3}} \gg 1$ and $\beta \gg 1$

This asymptotic regime has been discussed above and has also been studied previously by HB by a short-wave perturbation scheme.

(ii) $(\alpha R)^{\frac{1}{3}} \ll 1$ and $\beta \ll 1$

This gives rise to the long-wavelength perturbation scheme first devised by Yih (1967) for the channel configuration of two superposed viscous fluids and adapted by Hooper (1985) for the flow configuration of figure 1. The growth rate of the instability is found to be proportional to $(1-m)$ and so the flow is stable if the film of fluid is the less viscous fluid ($m > 1$) and unstable otherwise.

(iii) $(\alpha R)^{\frac{1}{3}} \gg 1$ and $\beta \ll 1$

This is the asymptotic regime studied in §3 by the singular perturbation method. The asymptotic analysis of the secular equation in this regime is discussed further in §4.3.

(iv) $(\alpha R)^{\frac{1}{3}} \ll 1$ and $\beta \gg 1$

The nature of the instability in this regime turns out to be similar to the instability found in regime (i). Further details of the asymptotic analysis of the secular equation in this regime are found in §4.4.

4.3. *Asymptotic analysis in regime (iii)*

When $(\alpha R)^{\frac{1}{3}} \gg 1$ and $\beta \ll 1$, (4.2) reduces to (4.3). The solution of the unstable mode of (4.3) is given by

$$\kappa = \frac{1-m}{m}\frac{N_{11}}{\beta Q_{11}}, \tag{4.6}$$

which is equivalent to

$$c = \frac{1-m}{m\alpha}\frac{\int_0^1 \sinh \alpha t \, \mathrm{Ai}\,(\mathrm{e}^{-5\mathrm{i}\pi/6}\,(\alpha R)^{\frac{1}{3}}(t+c))\,\mathrm{d}t}{\int_0^1 \mathrm{e}^{\alpha t}\,\mathrm{Ai}\,(\mathrm{e}^{-5\mathrm{i}\pi/6}\,(\alpha R)^{\frac{1}{3}}(t+c))\,\mathrm{d}t}. \tag{4.7}$$

Numerical results suggest that for this mode c is real at leading order and $O(1)$. The Airy functions within the integrands of (4.7) can therefore be replaced when $(\alpha R)^{\frac{1}{3}} \gg 1$ by their asymptotic form,

$$\mathrm{Ai}\,(z) = \tfrac{1}{2}\pi^{-\frac{1}{2}} z^{-\frac{1}{4}} \exp\left(-\tfrac{2}{3}z^{\frac{3}{2}}\right) \sum_{n=0}^{\infty} d_n z^{-\frac{3}{2}} \quad \text{as } |z| \to \infty \tag{4.8}$$

where $|\arg(z)| < \pi$ (Abramowitz & Stegun (1965, 10.4.59)). We check that the argument of the exponential term has no stationary points and apply Watson's lemma to evaluate each integral in (4.7) when $(\alpha R)^{\frac{1}{3}} \gg 1$. In such a manner we find that c has the following asymptotic form when $(\alpha R)^{\frac{1}{3}} \gg 1$:

$$c = c_0 + \frac{1}{(\alpha R)^{\frac{1}{2}}} c_{11} + \frac{1}{\alpha R} c_{12}, \tag{4.9a}$$

where

$$c_0 = \frac{1-m}{m}\frac{\sinh \alpha}{\alpha\, \mathrm{e}^{\alpha}}, \tag{4.9b}$$

$$c_{11} = \frac{1-m}{m}\mathrm{e}^{-3\mathrm{i}\pi/4}\frac{e^{-2\alpha}}{(1+c_0)^{\frac{1}{2}}}, \tag{4.9c}$$

and

$$c_{12} = -\mathrm{i}\frac{(1-m)}{m}\mathrm{e}^{-2\alpha}\left[\frac{\frac{5}{4}+\frac{1}{2}(1-m/m)\,\mathrm{e}^{-2\alpha}+\alpha(1+c_0)}{(1+c_0)^2}\right]. \tag{4.9d}$$

The $O(\epsilon)$-terms in (4.3) also contribute to the series expansion in $(\alpha R)^{-\frac{1}{2}}$ of c. We find that at leading order, the $O(\epsilon)$-terms modify c by the addition of the term

$$\frac{1}{\alpha R} c_{21}, \tag{4.9e}$$

where

$$c_{21} = -2\mathrm{i}\alpha^2[(1+m)+(1-m)\,\mathrm{e}^{-2\alpha}]. \tag{4.9f}$$

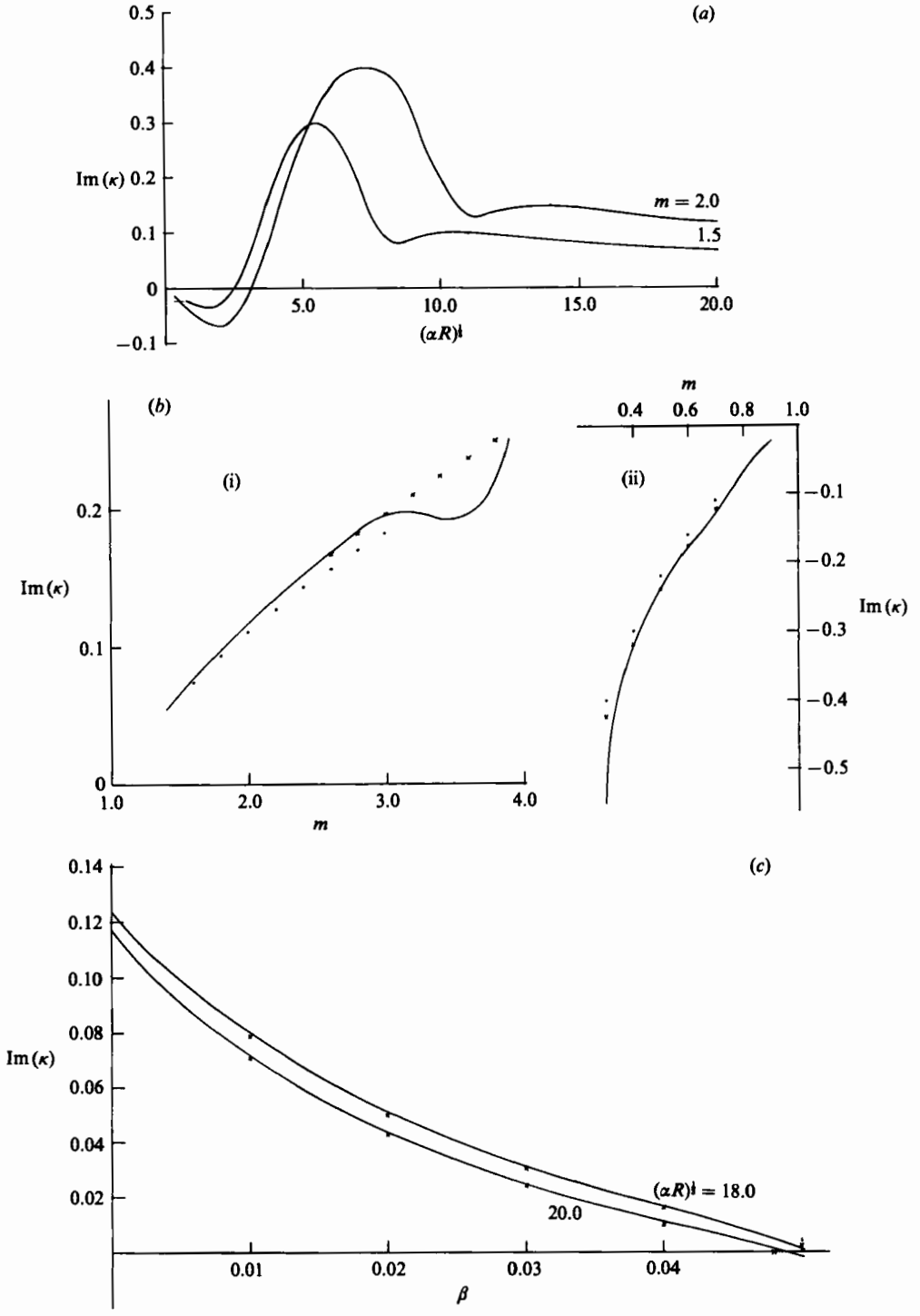

FIGURE 4. The unstable mode that arises when $m > 1$ with $(\alpha R)^{\frac{1}{3}} \gg 1$ and $\beta \ll 1$. (*a*) Im (κ) *vs.* $(\alpha R)^{\frac{1}{3}}$ when $\beta = 0$ and $m = 1{,}5, 2.0$: ·, the asymptotic form for Im (κ) of (4.9). (*b*) Im (κ) *vs.* m when $\beta = 0$ and (i) $(\alpha R)^{\frac{1}{3}} = 20.0$, $m > 1$; (ii) $(\alpha R)^{\frac{1}{3}} = 5.0$ $m < 1$. ·, the asymptotic form for Im (κ) of (4.9) up to $O(\alpha R)^{-\frac{1}{3}}$; ×, the asymptotic form for Im (κ) of (4.9) up to $O(\alpha R)^{-1}$. (*c*) Im (κ) *vs.* β when $m = 2.0$ and $(\alpha R)^{\frac{1}{3}} = 18, 20$. ×, the asymptotic form for Im (κ) of (4.9).

The expansion for c shown in (4.9) is in agreement with the results of §3. Numerical results for this mode are shown in figure 4. The asymptotic form for c is in good agreement with the numerical results for moderate values of m, large values of $(\alpha R)^{\frac{1}{3}}$ and small values of β.

4.4. *Asymptotic analysis in regime (iv)*

This regime is amenable to solution by either direct asymptotic evaluation of the secular equation or by a regular perturbation scheme applied to the governing equations of motion, (2.1), and the boundary conditions, (2.2) and (2.4). Both methods yield the same results and since the regular perturbation scheme is easier to implement, only this method will be described.

We rescale the equations of motion and boundary conditions using $\alpha y = z$ and hence solve the following system of equations:

$$\left(\frac{\mathrm{d}^2}{\mathrm{d}z^2}-1\right)^2 \phi_1(z) = \mathrm{i}\,\frac{1}{\beta^3}\,(z-\alpha c)\left(\frac{\mathrm{d}^2}{\mathrm{d}z^2}-1\right)\phi_1(z) \quad (-\alpha < z < 0), \tag{4.10a}$$

$$\left(\frac{\mathrm{d}^2}{\mathrm{d}z^2}-1\right)^2 \phi_2(z) = \mathrm{i}\,\frac{1}{\beta^3 m^2}\,(z-m\alpha c)\left(\frac{\mathrm{d}^2}{\mathrm{d}z^2}-1\right)\phi_2(z) \quad (z > 0), \tag{4.10b}$$

subject to

$$\phi_1(-\alpha) = 0, \tag{4.11a}$$

$$\phi_1'(-\alpha) = 0, \tag{4.11b}$$

$$\phi_2 \to 0 \quad \text{as } z \to \infty, \tag{4.12}$$

and the interfacial conditions at $y = 0$

$$\phi_1(0) = \phi_2(0) = \phi(0), \tag{4.13a}$$

$$\frac{\mathrm{d}\phi_1(0)}{\mathrm{d}z} = \frac{\mathrm{d}\phi_2(0)}{\mathrm{d}z} + \frac{\phi(0)}{c}\left(\frac{1-m}{m\alpha}\right), \tag{4.13b}$$

$$\left(\frac{\mathrm{d}^2}{\mathrm{d}z^2}+1\right)\phi_1(0) = m\left(\frac{\mathrm{d}^2}{\mathrm{d}z^2}+1\right)\phi_2(0), \tag{4.13c}$$

$$\left(\frac{\mathrm{d}^2}{\mathrm{d}z^2}-3\right)\frac{\mathrm{d}\phi_1(0)}{\mathrm{d}z} = m\left(\frac{\mathrm{d}^2}{\mathrm{d}z^2}-3\right)\frac{\mathrm{d}\phi_2(0)}{\mathrm{d}z} + \mathrm{i}\,\frac{1}{\beta^3}\,(\alpha^2 S)\,\frac{\phi(0)}{c}. \tag{4.13d}$$

Equation (4.22) can be solved by a regular perturbation method. Assume expansions for ϕ_j $(j = 1, 2)$ and c of the form

$$\phi_1(z) = \sum_{n=0}^{\infty} \epsilon^n \phi_{1n}(z), \tag{4.14a}$$

$$\phi_2(z) = \sum_{n=0}^{\infty} \epsilon^n \phi_{2n}(z) \tag{4.14b}$$

and

$$c = \sum_{n=0}^{\infty} \epsilon^n c_n, \tag{4.14c}$$

where

$$\phi_{1n}(z) = b_n(z)\,\mathrm{e}^{z} + d_n(z)\,\mathrm{e}^{-z}, \tag{4.14d}$$

$$\phi_{2n}(z) = a_n(z)\,\mathrm{e}^{-z} \tag{4.14e}$$

and

$$\epsilon = \beta^{-3} \ll 1. \tag{4.14f}$$

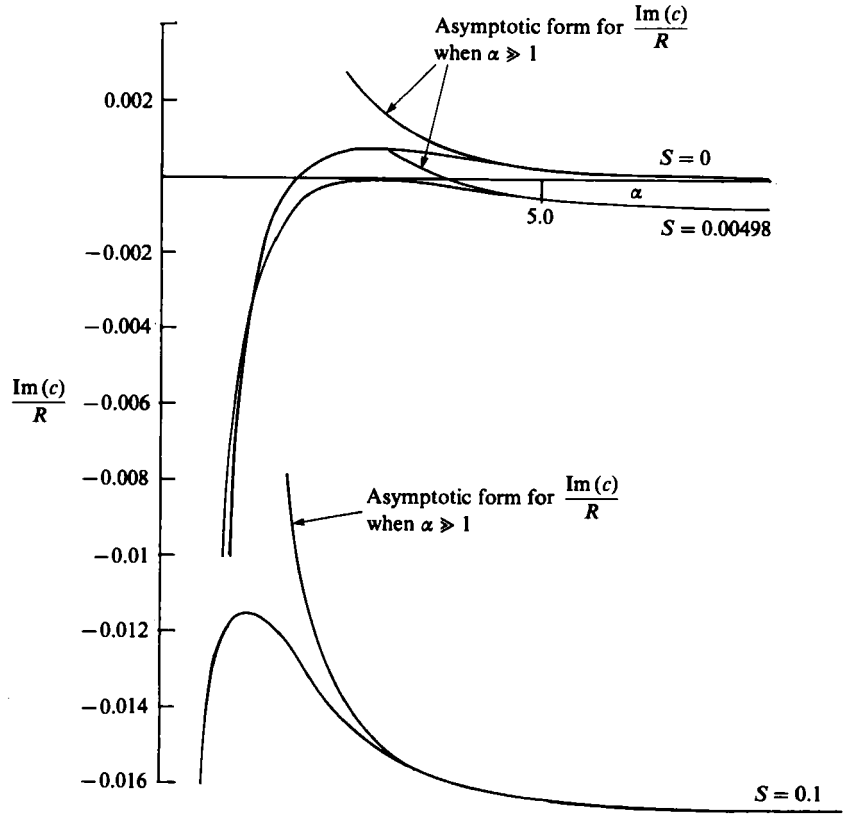

FIGURE 5. $(1/R)\,\mathrm{Im}(c)$ *vs.* α when $m = 2.0$ and $\beta \gg 1$ for different values of S. The upper branch shown at each value of S is the asymptotic form for $(1/R)\,\mathrm{Im}(c)$, which is

$$\frac{1}{2(1+m)\alpha^3}\left[\left(\frac{1-m}{m}\right)^2 - \alpha^3 S\right].$$

The items a_n, b_n and d_n are polynomials in z. We substitute these expansions for ϕ_1, ϕ_2 and c in (4.22)–(4.25). At $O(\epsilon^0)$ we find that

$$c_0 = \frac{4\alpha(1-m)}{\mathrm{e}^{2\alpha}(1+m)^2 + \mathrm{e}^{-2\alpha}(1-m)^2 + (1-m)(1+m)(4\alpha^2+2)}. \tag{4.15}$$

At $O(\epsilon)$ we find that c_1 is pure imaginary and when α is large, the expression for c_1 simplifies to

$$c_1 \sim \mathrm{i}\left[\frac{(1-m)^2}{2\alpha(1+m)m^2} - \frac{\alpha^2 S}{2(1+m)}\right].$$

The growth rate of the disturbance is equal to $(R/\alpha)c_1$ and is the same growth rate found by HB for the unbounded two-fluid problem. The value of $c_1/\alpha^2 (= \mathrm{Im}(c)/R)$ for any value of α is shown graphically in figure 5 for various values of dimensionless surface tension S. Figure 5 shows that when $S = 0$ the flow is stable below $\alpha = 1.8$ and unstable above $\alpha = 1.8$. This result indicates that on the $(\beta, (\alpha R)^{\frac{1}{3}})$-plane, one branch of the neutral stability curve asymptotes to the hyperbola $\alpha = \beta(\alpha R)^{\frac{1}{3}} = 1.8$ as β becomes large.

Table 1 shows the agreement between the analytical values for $\mathrm{Im}(\kappa)$, which are

	Analytical		Numerical	
	κ_r	κ_i	κ_r	κ_i
		(*a*) $\alpha = 1$, $m = 2.0$		
R				
0.2	−0.048095	−0.000636	−0.048134	−0.000563
0.1	−0.038173	−0.000250	−0.038181	−0.000224
0.01	−0.017718	−0.000116	−0.017720	−0.000011
		(*b*) $\alpha = 2$, $m = 2.0$		
R				
1.0	−0.023044	0.4676×10^{-3}	−0.023211	0.395×10^{-3}
0.1	−0.010696	0.2171×10^{-4}	−0.010697	0.18×10^{-4}
0.01	−0.004965	0.1007×10^{-5}	−0.004965	0.1×10^{-5}
		(*c*) $R = 1$, $m = 2.0$		
α				
2.0	−0.023044	0.4676×10^{-3}	−0.023211	0.395×10^{-3}
3.0	−0.004921	0.1087×10^{-3}	−0.005004	0.1077×10^{-3}
4.0	−0.000954	0.8175×10^{-3}	−0.000999	0.815×10^{-3}

TABLE 1. Comparison between analytical and numerical values for Im (κ)

equal to $(\alpha R)^{\frac{1}{3}}\beta^{-3}c_1$, and the numerical values for Im (κ), which are computed from (4.2) at small R. From figure 5 we also note that there is a critical value of S (0.00498) which stabilizes the flow at small R for all values of α.

5. Discussion

We have demonstrated that for the flow configuration of figure 1 there are three main types of instability which depend on the magnitude of the parameters $(\alpha R)^{\frac{1}{3}}$ and β. When $(\alpha R)^{\frac{1}{3}} \ll 1$ and $\beta \ll 1$ we find the Yih-type instability, which is only apparent if the lower bounded fluid is more viscous than the upper unbounded fluid. When $\beta \gg 1$ we find the short-wave instability of HB which occurs solely because of the presence of the interface. We have identified a third type of instability which exists in the regime $(\alpha R)^{\frac{1}{3}} \gg 1$ and $\beta \ll 1$. This instability arises at the viscous boundary layer at the wall and is only apparent when the kinematic viscosity of the lower bounded fluid is less than the kinematic viscosity of the upper unbounded fluid. The instability is confined to the lower less viscous fluid and the upper fluid remains relatively undisturbed.

Figure 6, which depicts the same neutral stability curve as figure 3 (*a*) but in the (α, R)-plane, where R is the Reynolds number of the lower fluid, shows that in the absence of surface tension, the flow of two fluids of equal density but with viscosity ratio $m = 2$ is unstable at all values of R. The numerical results depicted in figure 3 (*c*) and the asymptotic results shown in figure 5 reveal that surface-tension effects stabilize the flow at small R.

When $m < 1$, the flow configuration of figure 1 is still unstable when $\beta \gg 1$ and $(\alpha R)^{\frac{1}{3}} \gg 1$. This is the HB instability which arises in the absence of solid boundaries. The results of §4.4 show that this short-wave instability still exists when $(\alpha R)^{\frac{1}{3}} \ll 1$.

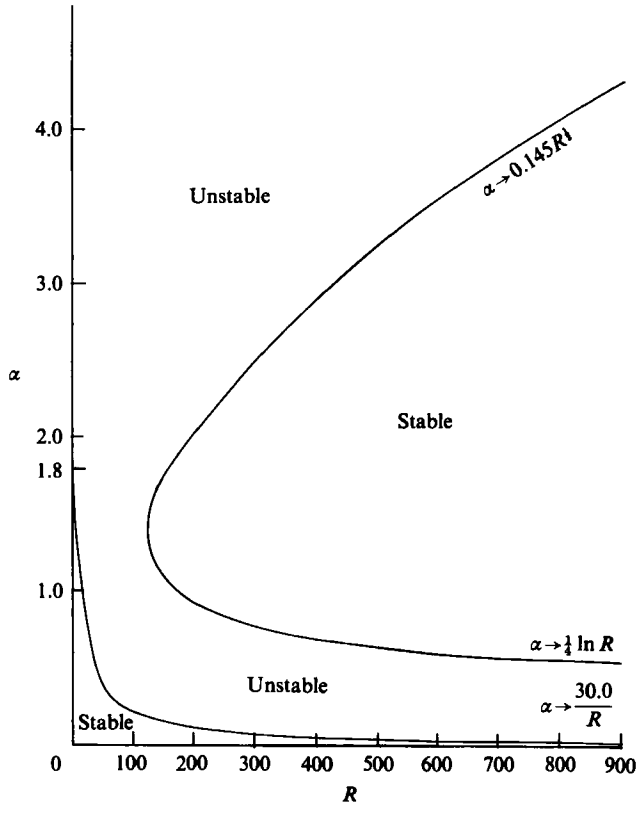

FIGURE 6. The neutral stability curve when $m = 2.0$ and $S_{HB} = 0$ in the (α, R)-plane. The asymptotic trend of each branch of the neutral stability curve is marked and stable and unstable regions are defined.

Asymptotic analysis yields that in the regime $\beta \ll 1$ and $(\alpha R)^{\frac{1}{3}} \ll 1$ the flow is unstable when $m < 1$ whereas when $\beta \ll 1$ and $(\alpha R)^{\frac{1}{3}} \gg 1$ the flow is stable. Thus the neutral stability curve for $m < 1$ is quite different from that for $m > 1$ when $(\alpha R)^{\frac{1}{3}}$ is small or β is small. Figure 7 (*a*) shows the neutral stability curve for the flow configuration of figure 1 with two fluids of equal density but viscosity ratio $m = 0.5$ in the $(\beta, (\alpha R)^{\frac{1}{3}})$-plane. Figure 7 (*b*) which is the same neutral stability curve but in the (α, R)-plane shows that this flow is unstable at all values of R.

The instability of §3, which arises when $m > 1$, $(\alpha R)^{\frac{1}{3}} \gg 1$ and $\beta \ll 1$, is characterized in figure 6 by the unstable region at large R between the two lower branches of the neutral stability curve. The results of §3.2 show that for fluids of unequal density the flow is unstable if the viscosity ratio $m(= \mu_2/\mu_1)$ is much greater than the density ratio $r(= \rho_2/\rho_1)$ and that the effect of surface tension and gravity on this instability is negligible. Therefore by interpreting the results of (3.32*c*) and (3.34) to extrapolate figure 6 to the case of two fluids of unequal density as well as unequal viscosity, we predict that an instability of moderate wavenumber α ($\sim d/\lambda$) should arise in the lower bounded fluid at high R of the flow provided that the kinematic viscosity of the lower fluid is less than the kinematic viscosity of the upper fluid.

Some experimental evidence for this instability may be found in the works of Charles & Lilleleht (1965) and Kao & Park (1972). Both studies were of plane Poiseuille flow of two superposed viscous fluids, namely oil and water, confined to

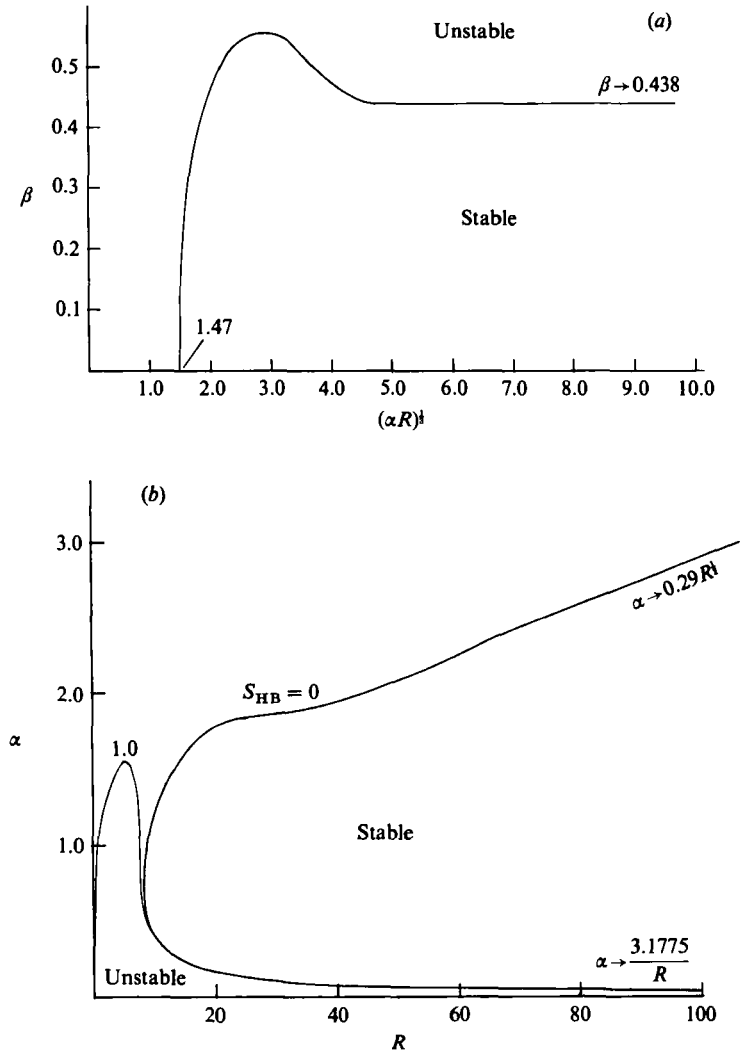

FIGURE 7. The neutral stability curve when $m = 0.5$ in the (*a*) $(\beta, (\alpha R)^{\frac{1}{3}})$-plane for $S = 0.0$; (*b*) (α, R)-plane for $S_{HB} = 0, 1.0$.

a channel. Both report an instability arising at high R of the less viscous fluid which causes the less viscous fluid to become unstable and the interface to become wavy but which does not affect the more viscous fluid. In particular Charles & Lilleleht report that for this instability the interfacial waves are approximately 0.5 in. long compared to a channel depth of 1 in. and that the ratio of oil Reynolds number to water Reynolds number is moderate. This implies a wavenumber α of approximately 2. These values of α and R together with a viscosity ratio $m = 5.3$ and a density ratio $r = 0.82$ suggest that this instability may be the instability studied in §3.

Poiseuille flow of one fluid confined to a channel is unstable at high R because of the presence of unstable Tollmien–Schlichting waves. The instability observed by Kao & Park and Charles & Lilleleht may be this unstable mode rather than the unstable interfaced mode discussed here. The mode that will be observed in practice is likely to be the one with the largest growth rate. The numerical results of figure 3

show that the growth rate of the unstable interfacial mode at non-zero values of surface tension is similar in magnitude to the growth rate of the unstable Tollmien–Schlichting wave of Poiseuille flow (see Rosenhead 1963, p. 531).

Hame & Muller (1975) have studied the stability of plane two-layer Poiseuille flow in the absence of surface tension. The flow configuration comprises a more viscous core fluid bounded by two thin layers of less viscous fluid next to the walls. Their results seem to indicate unstable Tollmien–Schlichting waves in Poiseuille flow rather than the unstable mode discussed in this paper. Blennerhassett (1980) studied the stability of various basic flows of two superposed viscous fluids in a channel. He discovered a variety of modes, some of which are surface modes and others shear modes. The results of his linear analysis indicates that the surface modes are the most unstable.

Finally it should be noted that the range of validity of the linear stability theory which at present is restricted to disturbance amplitude much less than the viscous lengthscale, can be greatly extended using curvilinear coordinates at the interface.

We wish to thank the referees for their many helpful comments. This work was supported by SERC grant GR/D/2417.3.

REFERENCES

Abramowitz, M. & Stegun, I. A. 1965 *Handbook of Mathematical Functions*. Dover.

Blennerhassett, P. J. 1980 On the generation of waves by wind. *Phil. Trans. R. Soc. Lond.* A **298**, 451.

Charles, M. E. & Lilleleht, L. U. 1965 An experimental investigation of stability and interfacial waves in co-current flow of two liquids. *J. Fluid Mech.* **22**, 217.

Dore, B. D. 1978*a* A double boundary-layer mode or mass transport in progressive interfacial waves. *J. Engng Maths* **12**, 289.

Dore, B. D. 1978*b* Some effects of the air–water interface on gravity waves. *Geophys. Astrophys. Fluid Dyn.* **10**, 215.

Drazin, P. G. & Reid, W. H. 1981 *Hydrodynamic Stability*. Cambridge University Press.

Hame, W. & Muller, U. 1975 On the stability of a plane two-layer Poiseuille flow. *Acta Mech.* **23**, 75.

Hinch, E. J. 1984 A note on the mechanism of the instability at the interface between two shearing fluids. *J. Fluid Mech.* **128**, 507.

Hooper, A. P. 1985 Long-wave instability at the interface between two viscous fluids: thin layer effects. *Phys. Fluids* **28**, 1613.

Hooper, A. P. & Boyd, W. G. C. 1983 Shear-flow instability at the interface between two viscous fluids. *J. Fluid Mech.* **128**, 507.

Kao, T. W. & Park, C. 1972 Experimental investigations of the stability of channel flows. Part 2. Two-layered co-current flow in a rectangular region. *J. Fluid Mech.* **52**, 401.

Renardy, Y. 1985 Instability at the interface between two shearing fluids in a channel. *Phys. Fluids* **28**, 3441.

Rosenhead, L. (ed) 1963 *Laminar Boundary Layers*. Oxford University Press.

Schulten, Z., Anderson, D. G. M. & Gordon, R. G. 1979 An algorithm for the evaluation of the complex Airy function. *J. Comp. Phys.* **31**, 60.

Yih, C.-S. 1967 Instability due to viscous stratification. *J. Fluid Mech.* **27**, 337.